Relationship between Membrane Physical Properties and Secretory Phospholipase A2 Hydrolysis Kinetics in S49 Cells during Ionophore-Induced Apoptosis

Rachel W. Bailey, Erin D. Olson, Mai P. Vu, Taylor J. Brueseke, Leslie Robertson, Ryan E. Christensen, Kristen H. Parker, Allan M. Judd, and John D. Bell
Department of Physiology and Developmental Biology, Brigham Young University, Provo, Utah

ABSTRACT During apoptosis, changes occur in lymphocyte membranes that render them susceptible to hydrolysis by secretory phospholipase A_2 ($sPLA_2$). To study the relevant mechanisms, a simplified model of apoptosis using a calcium ionophore was applied. Kinetic and flow cytometry experiments provided key observations regarding ionophore treatment: the initial rate of hydrolysis was elevated at all enzyme concentrations, the total amount of reaction product was increased fourfold, and adsorption of the enzyme to the membrane surface was unaltered. Analysis of these results suggested that susceptibility during calcium-induced apoptosis is limited by availability of substrate rather than adsorption of enzyme. Fluorescence experiments identified three membrane alterations during apoptosis that might affect substrate access to the $sPLA_2$ active site. First, intercalation of merocyanine 540 into the membrane was improved, suggesting an increase in lipid spacing. Second, laurdan detected increased solvation of the lower headgroup region of the membrane. Third, the rate at which fluorescent lipids could be removed from the membrane by albumin was enhanced, implying greater vertical mobility of phospholipids. Thus, it is proposed that the membranes of apoptotic cells become susceptible to $sPLA_2$ through a reduction in lipid-neighbor interactions that facilitates migration of phospholipids into the enzyme active site.

INTRODUCTION

Apoptosis is a complex process involving numerous alterations to components of the nucleus, cytoplasm, and cell membrane (1,2). Changes occurring at the cell membrane include exposure of phosphatidylserine, ceramide production, microvesicle shedding, membrane blebbing, loss of membrane potential, alterations to cytoskeletal attachments, and loss of membrane integrity (1–9). One of the earliest membrane events documented thus far is a substantial increase in the action of secretory phospholipase A_2 ($sPLA_2$) to hydrolyze plasma membrane lipids (9,10).

$sPLA_2$ has been used extensively for studying enzymatic activity at the water-membrane interface. A key feature of this enzyme is its ability to distinguish between healthy cells, which resist hydrolysis by $sPLA_2$, and damaged, necrotic, or apoptotic cells, which are often susceptible. Studies with artificial bilayers have demonstrated that the extent to which phospholipids are hydrolyzed by the enzyme depends on specific physical properties associated with the membrane (11–17). It has been proposed that analogous properties also govern the susceptibility of cell membranes (18–21).

A variety of experimental approaches has led to a general concept in which the action of $sPLA_2$ on the membrane surface involves at least two precatalytic steps (11,12,22–26). In the first step, $sPLA_2$ adsorbs to the membrane surface, and in the second, an individual phospholipid migrates into the active site of the enzyme (Scheme 1). In previous studies, this two-step hypothesis was examined using human erythrocytes as a simplified model for cell membranes (21). For those investigations, the apoptotic state of the cell was mimicked by treatment with ionomycin, a calcium ionophore. The resulting calcium influx produced changes in membrane structure accompanied by increased susceptibility to hydrolysis by $sPLA_2$. Analysis of these observations generated the conclusion that the ability of $sPLA_2$ to attack cell membranes is determined primarily by the ease of vertical migration of phospholipids into the active site of adsorbed enzyme (i.e., the second step in Scheme 1).

This foundational work from various membrane models has thus generated a testable hypothesis relating bilayer structure and $sPLA_2$ activity. The ultimate goal is a complete understanding of the biophysical and molecular principles governing this relationship in physiological and pathological settings such as apoptosis. Accomplishing this goal requires experiments with nucleated cells. Given the complexities associated with both apoptosis and cellular models for biophysical studies, we sought an experimental system in which measured effects would be maximized, the relationship between $sPLA_2$ activity and apoptotic markers would be known, and links to previous mechanistic studies would be plausible. Accordingly, S49 lymphoma cells treated with calcium ionophore (ionomycin) were chosen because they meet these criteria. Ionomycin stimulates rapid apoptosis that appears synchronized for the majority of the cell population resulting in large and reproducible changes in measured events.

Submitted January 17, 2007, and accepted for publication May 25, 2007.

Address reprint requests to John D. Bell, 302C WIDB, Brigham Young University, Provo, UT 84602. Tel.: 801-422-2353; Fax: 801-422-0050; E-mail: John_bell@byu.edu.

Editor: Antoinette Killian.

0006-3495/07/10/2350/13 $2.00

doi: 10.1529/biophysj.107.104679

$$E + M_S \underset{}{\overset{K_A}{\rightleftharpoons}} E_B \underset{Ca^{2+}}{\overset{K_E\ S}{\rightleftharpoons}} E_B{}^S \xrightarrow{k_{cat}} E_B + P$$

SCHEME 1 Reaction scheme for interaction between $sPLA_2$ and cell membranes. E, free $sPLA_2$; E_B, $sPLA_2$ adsorbed to membrane surface sites (M_s); S, available substrate (membrane phospholipid); E_B^s, adsorbed enzyme with substrate bound to the active site; K_A, equilibrium constant for enzyme adsorption to the membrane; K_E, equilibrium constant for substrate migration into the enzyme active site; k_{cat}, turnover number for substrate hydrolysis; P, product (fatty acid).

Moreover, as in human erythrocytes, the drug induces susceptibility to $sPLA_2$ that, in S49 cells, occurs with or before other major apoptotic changes (9,27).

The monomeric aspartate-49 phospholipase A_2 from the venom of *Agkistrodon piscivorus piscivorus* was used as the source of enzyme for several reasons. First, it has been used extensively in previous mechanistic and structural investigations, including studies with erythrocytes and S49 cells (9,11,15–21,23,25,27,28). Second, it is easily purified in large quantities, making it amenable to biophysical experiments. Third, it behaves similarly to some of the human isoforms of the enzyme during ionomycin-stimulated apoptosis (27).

Experiments were designed to examine each of the parameters shown in Scheme 1 to assess which is/are involved in distinguishing resistant cells from those treated with ionophore. This assessment was accomplished through measurements and analysis of hydrolysis kinetics, enzyme adsorption, and membrane structure. The results demonstrated that modulation of the second step (K_E in Scheme 1) accounts for the increased susceptibility to $sPLA_2$.

MATERIALS AND METHODS

Reagents

The monomeric aspartate-49 phospholipase A_2 from the venom of *A. p. piscivorus* was isolated according to the procedure by Maraganore et al. (29). Ionomycin was purchased from Calbiochem (La Jolla, CA) and dissolved in dimethylsulfoxide (DMSO) for experiments. The probes Oregon Green 488, 2-(6-(7-nitrobenz-2-oxa-1 3-diazol-4-yl)amino)hexanoyl-1-hexadecanoyl-*sn*-glycero-3 phosphocholine (NBD-PC), laurdan, acrylodan-labeled fatty acid-binding protein (ADIFAB), 1,3-bis-(1-pyrene)propane (bis-pyrene), diphenylhexatriene (DPH), merocyanine 540 (MC540), and propidium iodide were acquired from Invitrogen (Carlsbad, CA). Bovine serum albumin (BSA) was purchased from Sigma (St. Louis, MO). Other reagents were obtained from standard sources. Probes were dissolved in various solvents as follows: ADIFAB in 50 mM KCl and 3 mM NaN_3, bis-pyrene and DPH in N,N-dimethylformamide, NBD-PC in ethanol, and all others in DMSO.

Cell culture and experimental protocol

S49 mouse lymphoma cells were grown at 37°C in humidified air containing 10% CO_2 and prepared for experiments as described (28). Cell viability averaged 89 ± 6% (standard deviation). For spectral and kinetic experiments, an aliquot of cells (usually between 0.4×10^6 and 3.0×10^6 cells/ml in modified balanced salt solution (MBSS)) was then transferred to a quartz fluorometer sample cell and allowed 5 min to equilibrate in the spectrofluorometer (Fluoromax 3, Horiba Jobin-Yvon, Edison, NJ, or PC-1, ISS, Champaign, IL). Spectral bandpass varied between 4 and 16 nm depending on the intensity of the probe and instrument sensitivity. Data acquisition over time at multiple wavelengths (ADIFAB, laurdan, and bis-pyrene) was accomplished by rapid sluing of fluorometer mirrors under control of instrument software. Temperature and sample homogeneity were maintained as described previously (19). All experiments and incubations were performed at 37°C. For enzyme adsorption experiments, cells were resuspended in MBSS with 20 mM $BaCl_2$ to inhibit $sPLA_2$ hydrolytic activity without preventing adsorption (26,30,31).

In each procedure where ionomycin was added to cell samples (300 nM final), the experiment was repeated with an equivalent volume of DMSO (0.25% v/v final) to control for the effects of the solvent. A control for direct effects of ionomycin was also included in assessments of membrane physical properties (see below).

Membrane hydrolysis

Release of free fatty acids from cell membranes was assayed in real time with the fatty acid binding protein ADIFAB (excitation, 390 nm; emission, 432 nm and 505 nm). After initiating data acquisition for 100 s, ADIFAB (65 nM final) and ionomycin were added. At 700 s, $sPLA_2$ (0.7–70 nM final) was added and the time course continued for an additional 800 s. Raw data were quantified by calculating the generalized polarization (GP) and fitting to an arbitrary function by nonlinear regression (19). In some cases, hydrolysis was assayed by measurement of the rate of propidium iodide (37 μM final) uptake by cells due to the action of $sPLA_2$ as described (28). Previous experiments have demonstrated that assays with ADIFAB and propidium iodide give identical results under conditions at which cells are susceptible to the enzyme's catalytic activity (28). Thus, the propidium iodide assay was used only in experiments in which all samples were treated with ionomycin.

Enzyme adsorption

Adsorption of $sPLA_2$ to the cell surface was assayed by flow cytometry with Oregon Green 488-labeled $sPLA_2$ (L-PLA_2). Enzyme labeling was accomplished according to instructions provided with the kit (Invitrogen, Carlsbad, CA). Flow cytometry data were collected using a BD FACSCanto flow cytometer (BD Biosciences, San Jose, CA) with an argon excitation laser (excitation 488 nm, longpass 502 nm, bandpass filter 515–545 nm). Aliquots of cells (suspended in 1 ml MBSS containing 20 mM $BaCl_2$) were treated with ionomycin or DMSO for 10 min. For isotherm experiments, varying amounts of L-PLA_2 were then added (0.01–3 μM final), and samples were incubated for an additional 10 min before data acquisition. For competition experiments, samples were mixed with various concentrations of $sPLA_2$ (0.05–1 μM final) for 5 min before adding L-PLA_2 (50 nM final), and the incubation was continued for an additional 5 min. Samples were then immediately processed in the flow cytometer.

Probes of membrane structure

In addition to the ''vehicle control'' (DMSO), a control experiment was designed to verify that calcium entry into the cell, rather than artifacts resulting from direct effects of ionomycin, was responsible for the observed changes in membrane structure. This control involved incubation of the sample for at least 200 s with the calcium chelator ethylenediaminetetraacetic acid (EDTA) (18 mM final; the pH of the EDTA stock was adjusted to 7.6 at 37°C to avoid altering sample pH) before addition of ionomycin. In every case, the results from this ''EDTA control'' were indistinguishable from those obtained with the vehicle control. Hence, data from both types of controls are pooled in the presentation of results.

Data with MC540 (170 nM final) were acquired as emission spectra (excitation, 540 nm; emission, 550–700 nm). Spectra were obtained before the addition of the probe, after equilibration (5 min), and 10 min after addition

of ionomycin or control reagent(s). Spectra were analyzed by subtracting the initial spectrum as background and integrating the intensity from 565 to 615 nm. Effects of experimental treatments were quantified by calculating the difference in integrated intensity before and after treatment. That difference was divided by the integrated intensity before treatment to account for variations in cell number and lamp intensity. Changes in the wavelength of peak intensity were identified from derivatives of the spectra.

Laurdan or bis-pyrene fluorescence emission was acquired at dual wavelengths in real time. After initiating data acquisition, laurdan (50 nM final; excitation, 350 nm; emission 435 and 500 nm) or bis-pyrene (2.2 μM final; excitation, 344 nm; emission 376 and 480 nm) was added at 100 s. Ionomycin or control reagent(s) was/were included after initial equilibration of cells with the probe (laurdan, 10 min; bis-pyrene, 30 min). The laurdan GP and bis-pyrene excimer (480 nm)/monomer (376 nm) ratio were calculated from the data as described (19,32). Background intensity at each wavelength was subtracted from the data before calculations were made. For two-photon excitation microscopy of laurdan fluorescence, the concentration was increased to 250 nM to improve image distinction compared to background.

Data for steady-state anisotropy (DPH; excitation, 350 nm; emission, 452 nm) were acquired using Glan-Thompson polarizers in the vertical and horizontal positions. Data were obtained before the addition of the probe to measure background cell fluorescence, after 20 min equilibration with DPH (240 nM final), and 10 min after addition of ionomycin or control reagent(s). Anisotropy was calculated as described (33).

Phospholipid extraction

The fluorescent phospholipid analog, NBD-PC, was suspended in MBSS immediately before the experiments, as described by Jensen et al. (21). Cell samples were incubated with ionomycin or control reagent(s) (as in previous section) for 5 min. NBD-PC (930 nM final) was then introduced and allowed to incorporate into cell membranes (~30 min). After this incubation, cells were washed to remove excess probe. Data acquisition (excitation, 485 nm; emission, 535 nm) was then initiated, and BSA (0.7% final) was added for NBD-PC extraction. Apparent extraction-rate constants were obtained by fitting the fluorescence intensity data after BSA addition to a double exponential decay function by nonlinear regression.

Two-photon excitation scanning microscopy

Scanning two-photon excitation microscopy images were obtained using an Axiovert 35 inverted microscope (Zeiss, Thornwood, NY) at 37°C at the Laboratory for Fluorescence Dynamics (University of California, Irvine) as described previously (19,34). Laser emission was 940 nm for NBD-PC and 790 nm for Oregon Green 488. For laurdan (250 nM), dual images were collected simultaneously using a beam-splitter and interference filters (Ealing 490 and Ealing 440) with laser emission of 790 nm.

RESULTS

Hydrolysis kinetics

Addition of $sPLA_2$ to S49 cells previously exposed (10 min) to a control vehicle (DMSO) caused a slight increase in ADIFAB GP followed by a gradual decline, nearly restoring the value to its original level (Fig. 1, *curve a*). This unusual hydrolysis time course has been shown to represent transient initial hydrolysis followed by reacylation of the lipids and reincorporation into the membrane (27). In contrast, prior exposure of cells to ionomycin resulted in a large increase in ADIFAB GP that quickly reached a stable plateau (Fig. 1, *curve b*).

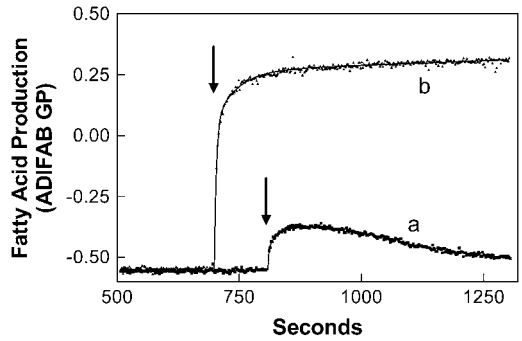

FIGURE 1 Effects of ionomycin treatment on the time course of membrane hydrolysis by $sPLA_2$. S49 cells were incubated with ADIFAB and treated for at least 600 s with DMSO (*curve a*) or ionomycin (*curve b*) as explained in Materials and Methods. At the time indicated by the arrows, $sPLA_2$ (70 nM final) was added. Data points represent the raw data (expressed in GP units), and curves represent nonlinear regression fits of the data using an arbitrary function consisting of the sum of two exponential functions. The amount of hydrolysis observed in *curve a* constitutes ~2–5% of the plasma membrane phospholipid (27).

To further characterize hydrolysis kinetics, the experiment in Fig. 1 was repeated at various enzyme concentrations. Data were analyzed by nonlinear regression (examples are shown in Fig. 1). From these phenomenological fits, two parameters were determined: the initial rate of hydrolysis and maximum hydrolysis product generated. As displayed in Fig. 2, treatment of cells with ionomycin increased both initial and total hydrolysis at all enzyme concentrations. The maximum hydrolysis rate was 0.018 ± 0.004 GP units s^{-1} for DMSO-treated samples and 0.093 ± 0.011 GP units s^{-1} for the ionomycin group. The enzyme concentration at which the hydrolysis rate was one-half the maximum was 13.5 ± 7.8 nM and 9.4 ± 3.2 nM, respectively, for the two groups. Two-way analysis of variance indicated that both the effects of enzyme concentration and ionomycin treatment on the initial hydrolysis rate were highly significant ($p < 0.0001$). A significant interaction ($p < 0.0001$) between the two variables was also observed, suggesting that the magnitude of the effect of ionomycin depended on enzyme concentration. The ability of ionomycin treatment to increase total hydrolysis product was also significant ($p < 0.0001$).

Enzyme adsorption

Initial attempts to quantify adsorption of $sPLA_2$ to the cell surface involved a conventional centrifugation assay with fluorescent-labeled enzyme (L-PLA_2), as done previously with erythrocytes (21). However, control experiments suggested that the observed association of enzyme with the cells was not reversible. Analysis of microscopy images indicated that this irreversible interaction reflected endocytosis of the labeled enzyme, a phenomenon previously described for nucleated cells (35–37).

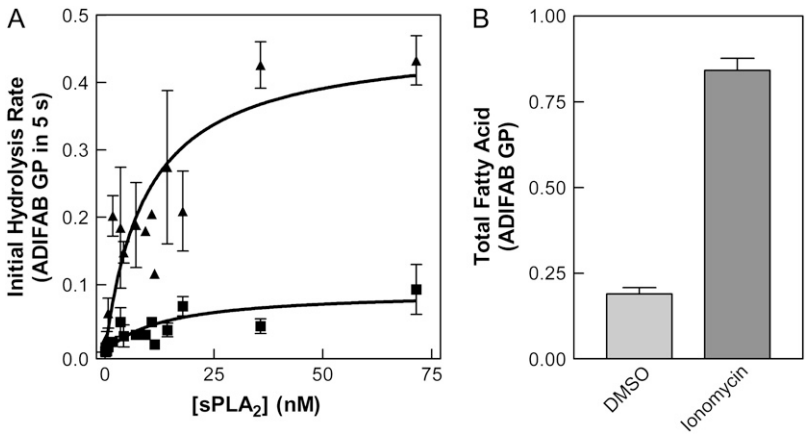

FIGURE 2 $sPLA_2$ concentration dependence of the initial rate of hydrolysis. (*A*) The experiments of Fig. 1 were repeated at the indicated concentrations of $sPLA_2$ for cells treated with DMSO (*squares*) or ionomycin (*triangles*). The initial rate was defined as the amount of product generated during 5 s from the time of enzyme addition. This number was calculated from nonlinear regression fits of the data, as shown in Fig. 1. Data were analyzed by two-way analysis of variance to assess the contribution of $sPLA_2$ concentration (37% of variation, $p < 0.0001$), ionomycin treatment (13% of variation, $p < 0.0001$), and the interaction between the two (20% of variation, $p < 0.0001$). Data points represent the raw data (expressed in GP units), and curves represent nonlinear regression fits of the data using an arbitrary function. (*B*) The total amount of product after 600 s (or at the maximum for time courses shaped like that of *curve a* in Fig. 1) for enzyme concentrations $\geq$18 nM. The data were significant based on two-tailed unpaired Student's *t*-test ($p < 0.0001$, $n = 1$–4 at each datum).

Flow cytometry experiments were designed to distinguish endocytosis of labeled enzyme from reversible adsorption to the cell surface. Cells were treated with ionomycin or DMSO for 5 min. All samples were then mixed with L-PLA_2, and half of the samples were washed to remove free enzyme. Fig. 3 displays histograms of L-PLA_2 fluorescence intensity per cell in each of these four groups. Most of the data from DMSO-treated samples appeared to originate from a single population of cells (Fig. 3 *A*). The intensity of this group was reduced 10-fold (i.e., one log unit along the abscissa) by washing (Fig. 3 *C*), suggesting that this peak represented reversible adsorption of L-PLA_2 to the cell exterior. In unwashed ionomycin-treated samples (Fig. 3 *B*), at least two distinct populations were identified in the histogram of fluorescence intensity. Cells with low fluorescence intensity (Fig. 3 *B*, *left arrow*) accounted for a majority of the sample, yet they only contributed ~20% of the total fluorescence signal. The fluorescence of this population was also reduced 10-fold by washing, similar to the DMSO-treated cells (Fig. 3 *D*, *left arrow*). In contrast, the high intensity staining was less affected by washing (Fig. 3, *B* and *D*, *right arrow*), suggesting that this staining represented internalization of the enzyme (35–37). This irreversibility corroborated observations from two-photon microscopy (not shown; see previous paragraph). Given that reversible surface adsorption is the relevant phenomenon for interpreting the hydrolysis kinetics, we focused our analysis on the low-intensity population.

Fig. 4 displays the amount of reversible surface adsorption of various concentrations of L-PLA_2. The average apparent equilibrium constant for adsorption of L-PLA_2 to DMSO-treated cells was $2.5 \times 10^6\ M^{-1}$. There was no detectable effect of ionomycin treatment on either the apparent equilibrium constant ($1.7 \times 10^6\ M^{-1}$, $p = 0.39$) or the maximum number of adsorption sites per cell ($p = 0.20$).

To relate these adsorption results to native $sPLA_2$, competition experiments were performed. Unlabeled $sPLA_2$ competed for ~30–40% of the L-PLA_2 adsorption sites at all concentrations within the range tested (0.05–1 μM $sPLA_2$ with 50 nM L-PLA_2). This result suggested that more than half of these adsorption sites might not be relevant to hydrolysis by $sPLA_2$. The observation that competition was already maximal when the same concentrations of $sPLA_2$ and L-PLA_2 were used (50 nM) indicated that the enzyme adsorbs more tightly when it is not labeled. This inference is consistent with the relatively high potency of the unlabeled enzyme shown in Fig. 2.

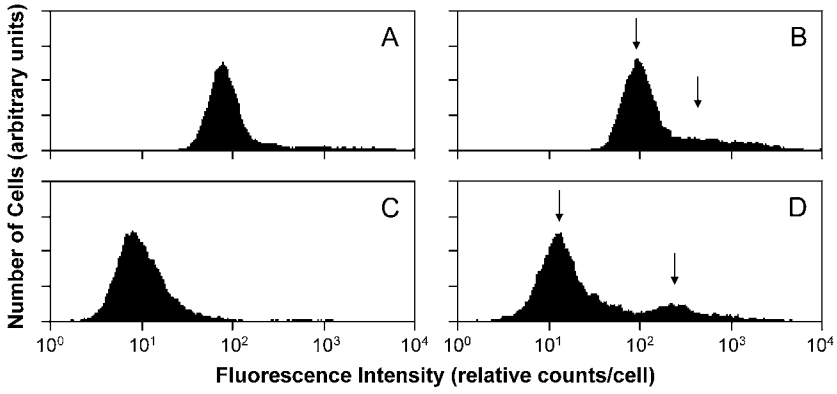

FIGURE 3 Reversibility of adsorption of L-PLA_2 to S49 cells. Data represent histograms for Oregon Green fluorescence intensity obtained by flow cytometry, as explained in Materials and Methods. (*A* and *B*) Cells were treated with DMSO (*A*) or ionomycin (*B*) for 5 min followed by 5 min incubation with 1 μM L-PLA_2. Samples were then transferred immediately to the flow cytometer. (*C* and *D*) The experiments in *A* (*C*) and *B* (*D*) were repeated as stated, except that cells were separated from the supernatant by centrifugation and washed in fresh MBSS with 20 mM $BaCl_2$ before flow cytometry. In *B* and *D*, the left arrow indicates the low-intensity, reversible staining of cells with L-PLA_2, and the right arrow indicates the high-intensity staining that was not removed by washing (explained in Results).

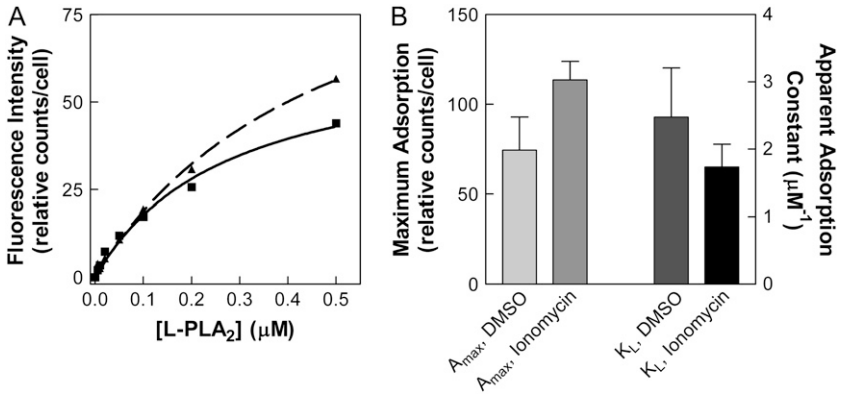

FIGURE 4 Concentration dependence of L-PLA_2 adsorption to S49 cells. (*A*) The experiments of Fig. 3, *A* and *B*, were repeated at the indicated concentrations of L-PLA_2. The amount of adsorbed L-PLA_2 was estimated from the fluorescence intensity represented by the mode of the low-intensity peak in the flow cytometry histograms (e.g., as indicated in Fig. 3 *B* (*left arrow*)). Data (*squares*, DMSO; *triangles*, ionomycin) were fit by nonlinear regression to a standard Langmuir binding isotherm function. (*B*) Values for an apparent adsorption constant (K_L) and the maximum adsorption at saturation (A_{max}) were obtained from fits such as those shown in *A* for four independent experiments. The data for DMSO and ionomycin-treated samples were compared by two-tailed paired Student's *t*-test. Adsorption constant: $p = 0.39$; maximum adsorption: $p = 0.20$. Data are expressed as mean ± SE.

To better estimate the apparent adsorption constant for unlabeled $sPLA_2$ (K_{app}), we took advantage of control observations (not shown) demonstrating that L-PLA_2 is a weak enzyme (possessing ≤1/10 the activity of $sPLA_2$). Accordingly, we repeated the competition experiments using a hydrolysis assay at constant $sPLA_2$ concentration (70 nM final, E_T in Eq. 1) in the presence of various amounts of L-PLA_2 (0.05–20 μM final, L_T in Eq. 1). The initial hydrolysis rate data (dP/dt) were fit to the following equation with α as an arbitrary proportionality constant:

$$\frac{dP}{dt} = \frac{\alpha K_{app} E_T}{1 + K_{app} E_T + K_L L_T}. \quad (1)$$

We assumed that K_L, the adsorption constant for L-PLA_2, was the same at sites of hydrolysis as that estimated for the entire cell in Fig. 4. Results shown in Fig. 5 provide convincing evidence for competition. Analysis of the data by nonlinear regression estimated that K_{app} equals 2.7×10^7 M^{-1}.

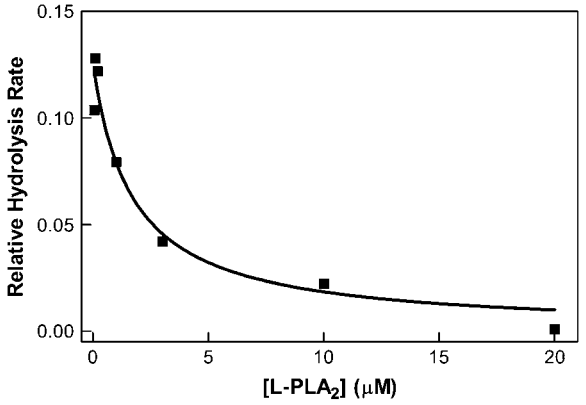

FIGURE 5 Ability of L-PLA_2 to interfere with cell membrane hydrolysis by $sPLA_2$. Cells were treated for 400 s with ionomycin and then subjected to hydrolysis by 70 nM $sPLA_2$. Hydrolysis was assayed using propidium iodide (see Materials and Methods). The relative hydrolysis rate was calculated as the inverse of the half-time for uptake of propidium iodide by the cells (28). The experiment was repeated in the presence of the indicated concentrations of L-PLA_2. The data were fit by nonlinear regression to Eq. 1 as described in Results.

Physical changes in the cell membrane

Previous experiments with erythrocytes revealed several physical changes in the cell membrane that appeared to explain the basis for increased susceptibility to the action of $sPLA_2$. These included increases in the spacing among bilayer lipids, the average level of lipid order, and the rate at which fluorescent phospholipids could be extracted from the cell membrane (21). Similar experiments have been included here to test the relevance of those findings to nucleated cells.

Phospholipid spacing

Changes in phospholipid spacing were assessed with MC540, a probe that intercalates between the phospholipid heads in the outer leaflet of cell membranes (38–40). Treatment of cells with ionomycin resulted in a significant increase in MC540 total fluorescence (Fig. 6 *A*) and a red-shift in peak wavelength from ~583 to 586 nm (Fig. 6 *B*), consistent with increased binding of the probe (41). As shown in Fig. 6, *C* and *D*, these effects were reproducible. Control experiments in which cells were treated with ionomycin in the presence of a calcium chelator (EDTA) demonstrated that these effects were due to calcium influx rather than representing artifacts caused directly by the presence of ionomycin in the membrane. Since EDTA controls were indistinguishable from DMSO-treated samples, data from both types of controls were pooled in the presentation of results for MC540 and all other probes of membrane physical properties (see legends to Figs. 6–9). These spectral changes in MC540 fluorescence suggest that treatment with ionomycin increased the spacing among membrane phospholipids.

Membrane order

Three fluorescent probes were used to examine the relationship between susceptibility and membrane order. Laurdan

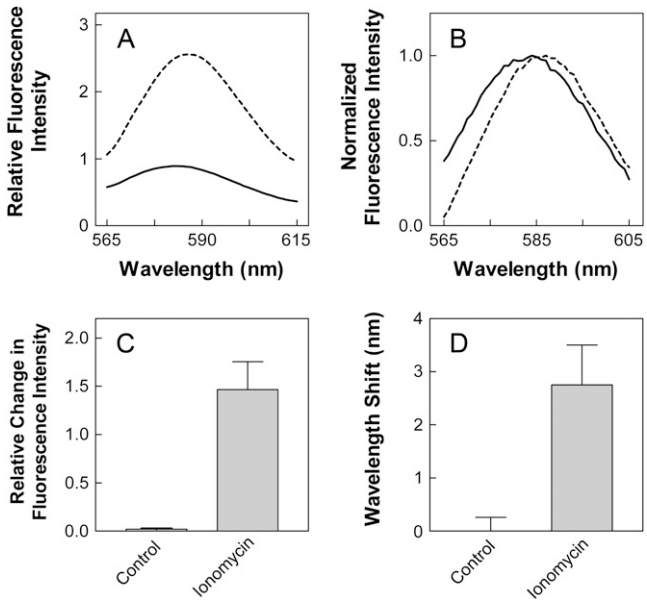

FIGURE 6 Effects of ionomycin treatment on MC540 fluorescence. (*A*) Representative emission spectra showing the intensity of MC540 bound to S49 cells before (*solid curve*; labeling details explained in Materials and Methods) and 10 min after ionomycin addition (*dashed curve*). (*B*) Spectra displayed in *A* were normalized to their respective maximum intensities. (*C* and *D*) The change in MC540 fluorescence intensity (*C*) (quantified as described in Materials and Methods) and shift in wavelength of emission maximum (*D*) were compared for controls (vehicle and EDTA controls; see Materials and Methods) and ionomycin-treated samples by two-tailed unpaired Student's *t*-test. Data are expressed as mean ± SE. $p < 0.0001$ (*C*); $p = 0.005$ (*D*); $n = 6$ (controls) or 3 (ionomycin).

intercalates at the level of the glycerol backbones (42). The shape of laurdan's emission spectrum is highly sensitive to the solvent relaxation effect and is quantified as GP (see Materials and Methods). GP varies between −1.0 and 1.0 and has been interpreted to reflect the degree to which lipid molecules are ordered within the membrane (a value of 1.0 denotes a highly ordered membrane in which no solvent relaxation occurs (32,33)). Bis-pyrene has traditionally been used to evaluate the level of ''fluidity'' in the membrane, implying the ability of molecules to diffuse laterally along the bilayer plane (43). More recent experiments exploring the phosphatidylcholine/cholesterol phase diagram indicated that the probe is more sensitive to phospholipid acyl chain order (44). Presumably, bis-pyrene resides deep in the membrane, based on the partitioning of the parent compound, pyrene (45). Diphenylhexatriene also locates deep in the membrane (46). The anisotropy of DPH is sensitive to both fluidity (which alters the rotational diffusion rate of the probe) and environmental constraints imposed by the level of chain order (44,47).

Laurdan GP before and after treatment with ionomycin and subsequent controls is illustrated in Fig. 7. In Fig. 7 *A*, laurdan GP over time is displayed. Ionomycin (added at *arrow*) caused GP values to decrease until it reached a minimum 10 min after treatment. This effect was significant (Fig. 7 *B*). Images collected by two-photon microscopy verified that the changes reported in Fig. 7 *B* were confined to the plasma membrane (Fig. 7, *C–F*). In contrast, no differences in apparent lipid order were identified with either bis-pyrene excimer/monomer ratio or DPH steady-state anisotropy (Fig. 8).

Phospholipid extractability

Changes in the propensity of phospholipids to migrate vertically in the bilayer were estimated by extraction experiments utilizing NBD-PC, a fluorescent phospholipid analog that inserts into lipid bilayers (21,48). We used the protein BSA as a lipid acceptor in these experiments. This protocol allowed us to estimate the rate of extraction. As shown in Fig. 9 *A*, time courses of NBD-PC fluorescence after BSA addition were fit to a two-phase exponential decay (with $t = 0$ corresponding to the time of BSA addition), with a rapid initial drop in intensity followed by a gradual decline. An overall rate constant was derived from the regressions and compared for multiple samples (Fig. 9 *B*). Ionophore treatment generated a reproducible twofold increase in the rate of NBD-PC extraction.

Initial and final fluorescence intensities often differed between DMSO- and ionomycin-treated samples (generally greater in the ionophore group, not shown). For this reason, the data in Fig. 9 *A* are normalized. We used flow cytometry and two-photon microscopy to address the possibility that intensity differences reflected artifacts (due to the extent of extraction and/or labeling) that might interfere with our analysis. Flow cytometry experiments demonstrated that the amount of fluorophore removed by BSA was comparable between control and treatment groups (89% and 85%, respectively (not shown)). Two-photon microscopy images revealed that it was common for cells to display labeling of internal compartments in addition to the plasma membrane (more prominent in ionomycin-treated cells; example shown in Fig. 9, *C–E*). Upon BSA addition (between Fig. 9, *C* and *D*), fluorescence intensity decreased quickly from the perimeter of the cells and more gradually from the interior (Fig. 9 *D*, 2 min after addition; Fig. 9 *E*, 4 min after addition). These experiments convinced us that at least the initial rapid decay of fluorescence intensity, dominant in the analysis shown in Fig. 9, *A* and *B*, could reasonably be interpreted to represent lipid extraction from the cell membrane.

DISCUSSION

The purpose of this study was to identify how changes in the cell membrane induced by calcium ionophore treatment might increase the rate of phospholipid hydrolysis by extracellular $sPLA_2$. To this end, the model shown in Scheme 1 was used to analyze the results of the kinetic experiments displayed in Fig. 2. The initial rate of lipid catalysis (dP/dt) is given by

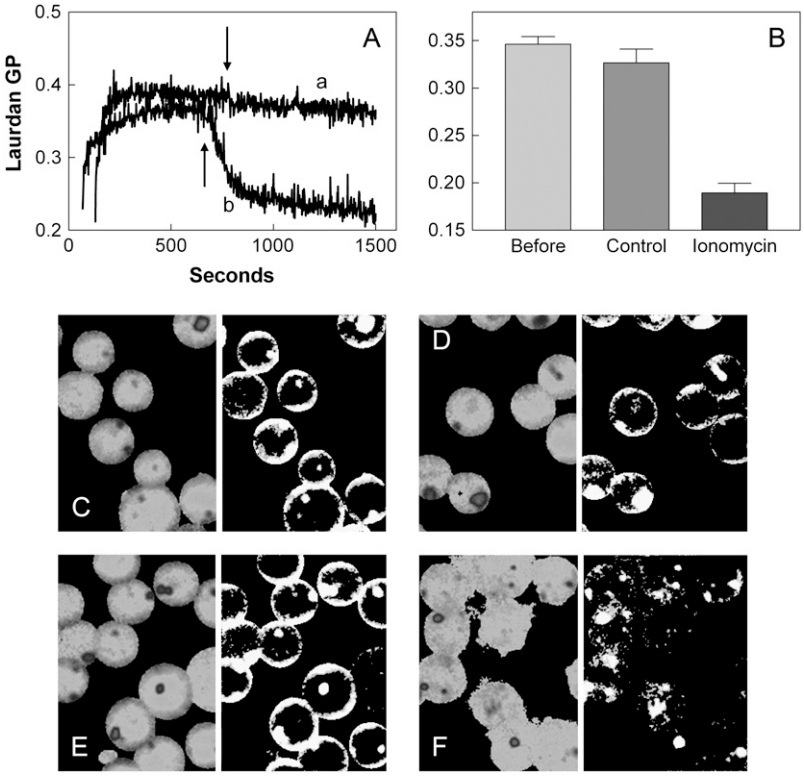

FIGURE 7 Effect of ionomycin on laurdan GP. (*A*) Cells labeled with laurdan were treated without (*curve a*, vehicle control) or with (*curve b*) ionomycin (*arrows*). (*B*) For each experiment, 30 points before treatment with ionomycin were averaged and pooled in the ''Before'' group ($n = 12$). ''Controls'' ($n = 6$) and ''Ionomycin'' ($n = 6$) groups represent the average of 30 points after stabilization of the fluorescence signal. Data are expressed as mean ± SE and analyzed by one-way analysis of variance with Bonferroni's Multiple Comparison Post Test ($p < 0.0001$ overall; Before versus Controls: $p > 0.05$; Before versus Ionomycin: $p < 0.001$; Controls versus Ionomycin: $p < 0.001$). (*C–F*) Two-photon images of S49 cells were collected before and after incubation with ionomycin in the absence or presence of EDTA (as a control): (*C*) EDTA; (*D*) EDTA + ionomycin; (*E*) normal calcium; (*F*) normal calcium + ionomycin. In each image, the left half displays a broad range of GP values from –0.1 (*white*) to 0.62 (*dark gray*), and the right half displays the same image with a basement threshold of 0.1, so that only pixels corresponding to high GP values are shown.

$$\frac{dP}{dt} = \frac{\beta K_A E_T K_E S_T}{1 + K_A E_T (1 + K_E S_T)}, \tag{2}$$

where β is proportional to k_{cat} and the total number of adsorption sites for the enzyme (E_T) (21). It is assumed that β does not change with experimental treatment because alterations to membrane structure would presumably affect reaction steps preceding the catalytic event (see Jensen et al. (21) and discussion below). For simplicity, β is assigned a value of 1.0 GP units s^{-1}. S_T represents the mole fraction of membrane phospholipids available to the enzyme. In previous analyses, it has not been considered separately from K_E since the two parameters are completely linked in the model (see Eq. 2 and Jensen et al. (21)). However, the data of Fig. 2 *B* demonstrate that S_T is subject to change upon experimental treatment and provide information to quantify the magnitude of that change. S_T is therefore included specifically as a parameter in Eq. 2 and expressed in relative units (i.e., it is assigned a value of 1.0 under control conditions).

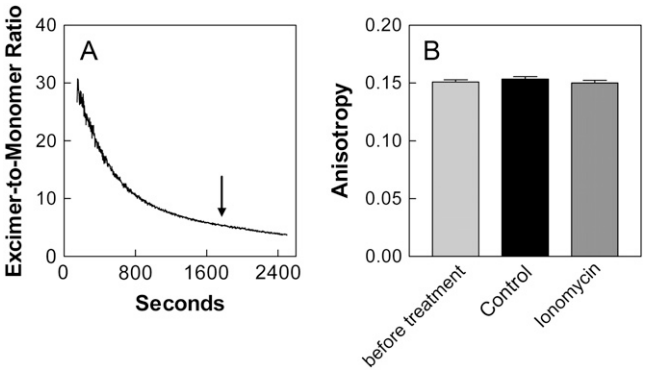

FIGURE 8 Effect of ionomycin on bis-pyrene and DPH fluorescence. (*A*) Time course of bis-pyrene excimer/monomer ratio; ionomycin was added at the *arrow*. (*B*) Cells were labeled with DPH as explained in Materials and Methods, and anisotropy measurements were obtained before ($n = 10$, all samples pooled) and after treatment with control reagent(s) ($n = 6$) or ionomycin ($n = 4$). Data are expressed as mean ± SE and were not significant based on one-way analysis of variance ($p = 0.61$).

As shown in Fig. 10 *A*, the control data from Fig. 2 *A* were well fit by Eq. 2. The value of K_A (6.7×10^7 M^{-1}) matched favorably the value estimated from competition with L-PLA_2 (2.7×10^7 M^{-1} in Fig. 5). The effect of ionomycin on the initial hydrolysis rate was evaluated by considering S_T, K_A, and K_E individually in the fit to identify the minimum criteria required by the results (parameter values summarized in Table 1). The data of Fig. 2 *B* indicated that S_T increased by a factor of ~4.4 with ionophore treatment. Accordingly, Eq. 2 was recalculated maintaining all parameter values from the fit of the control data with the exception of S_T. The 4.4-fold increase, however, was insufficient to account for the ionomycin data (Fig. 10 *B*). In fact, a reasonable fit was obtained only with a much larger (8.1-fold) increase in S_T, one that cannot be justified based on the data of Fig. 2 *B* (Fig. 10 *C*). Since K_E and S_T are linked in Eq. 3, the dilemma can obviously be resolved by increasing K_E by a factor of 1.8 in

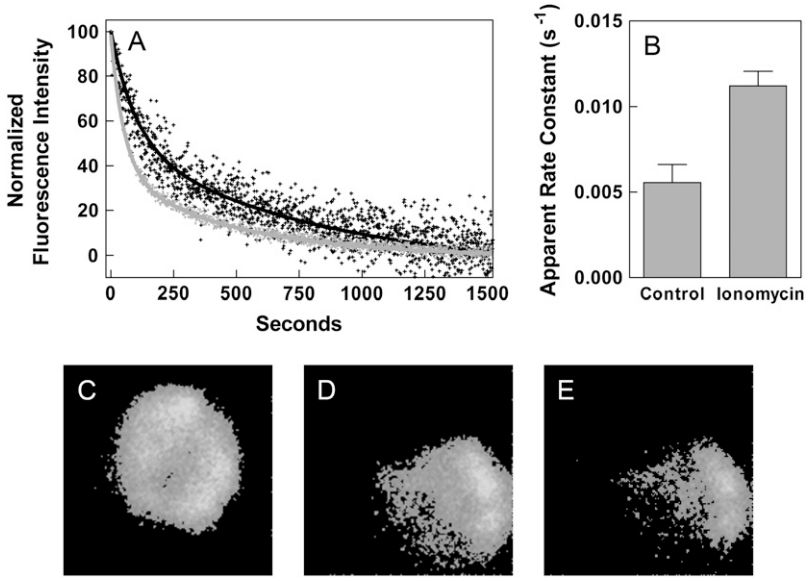

FIGURE 9 Effect of ionomycin on the rate of NBD-PC extraction by BSA. (*A*) Time course of NBD-PC fluorescence in samples treated with ionomycin (*gray*) or control reagent(s) (*black*) with $t = 0$ corresponding to the time of BSA addition. Data points are normalized to the maximum and minimum fluorescence intensity, and curves are two-phase exponential decay fits. (*B*) The rate constant obtained from these fits for controls ($n = 7$) and ionomycin-treated ($n = 5$) samples were compared by two-tailed unpaired Student's *t*-test. Data are expressed as mean ± SE ($p = 0.003$). (C–E) Two-photon images of an S49 cell labeled with NBD-PC and treated with ionomycin (*C*) before, (*D*) 2 min after, and (*E*) 4 min after addition of BSA.

addition to a fixed 4.4-fold increase in S_T (Fig. 10 *D*). Alternatively, allowing K_A to vary instead of K_E was inadequate to accommodate the data (Fig. 10 *E*). The best fit, of course, was obtained when both K_A and K_E were allowed to float in combination with the prescribed increase in S_T (Fig. 10 *F*). This ideal fit corresponded to a twofold increase in K_E (in strong agreement with that of Fig. 10 *D*) coupled with a reduction in K_A by ~16% (corroborating the result in Fig. 10 *E*). Thus, we concluded from this analysis that increased susceptibility after ionomycin treatment has little or nothing to do with the strength of adsorption (K_A) and can be explained entirely by increases in the accessibility of lipids to the enzyme active site (K_E and S_T).

It is important to note that the differences between control and treatment curves in Fig. 2 *A* could easily be explained by adjustments to k_{cat}. Variations in k_{cat} could be due to either cofactor availability or enzyme conformational change. Since the same medium was used in all data sets, availability of the cofactor calcium was not an issue. Moreover, if changes in membrane microstructure stabilized the transition to an activated enzyme conformation, that stabilization would be reflected by enhanced adsorption of $sPLA_2$ to the membrane surface. Although multiple conformations of $sPLA_2$ have indeed been observed and may be linked to adsorption and/or substrate binding (49), we have no evidence that adsorption of the enzyme is altered by ionomycin. Therefore, it is unlikely that conformational transitions are affected by ionophore treatment, and our use of a constant value for k_{cat} (i.e., the parameter "β" in Table 1 and Eq. 2) is appropriate.

It may seem surprising that the affinity of the enzyme to adsorb to the membrane surface (K_A) was not altered by ionomycin treatment (Fig. 4). It is well established that calcium influx promotes exposure of anionic phosphatidylserine on the outer surface of the cell membrane (50,51). In previous studies with ionophore-treated S49 cells, this lipid flip-flop occurred as early as could be detected and corresponded temporally with increased susceptibility to $sPLA_2$ activity (9). Moreover, the presence of anionic lipids greatly promotes $sPLA_2$ adsorption in artificial bilayers and cells (11,52–54). Since much of the adsorption of labeled-$sPLA_2$ observed in Fig. 4 appeared unrelated to membrane hydrolysis (for example, binding to heparin sulfate (55)), it could be argued that the methods employed to assess K_A were incapable of discerning relevant changes. For this reason, we applied the kinetic analysis detailed in Fig. 10, which substantiated the idea that differential membrane susceptibility is not determined by variation in enzyme adsorption. Furthermore, experiments in human erythrocytes with an inhibitor of phosphatidylserine translocation supported the conclusion that exposure of anionic lipids was not a requirement for enhanced hydrolysis upon ionomycin treatment (9,18). This view is supported by studies indicating that apoptotic stimuli other than ionomycin induced $sPLA_2$ susceptibility before phosphatidylserine exposure in S49 cells (9). Overall, these findings suggest that transbilayer movement of specific phospholipids does not necessarily provide a preferred substrate for the enzyme, nor is flip-flop the primary determinant of membrane vulnerability to $sPLA_2$. Nonetheless, loss of membrane asymmetry could possibly alter other properties of the phospholipid bilayer, which then render the membrane sensitive to $sPLA_2$ activity. For example, exposure of phosphatidylserine could contribute to the increased lipid spacing we observed (56).

A caveat to the conclusion that increased membrane susceptibility to $sPLA_2$ does not result from enhanced enzyme adsorption and/or flip-flop of phosphatidylserine is the fact that the experiments reported here were conducted with enzyme purified from snake venom. Several isoforms of $sPLA_2$

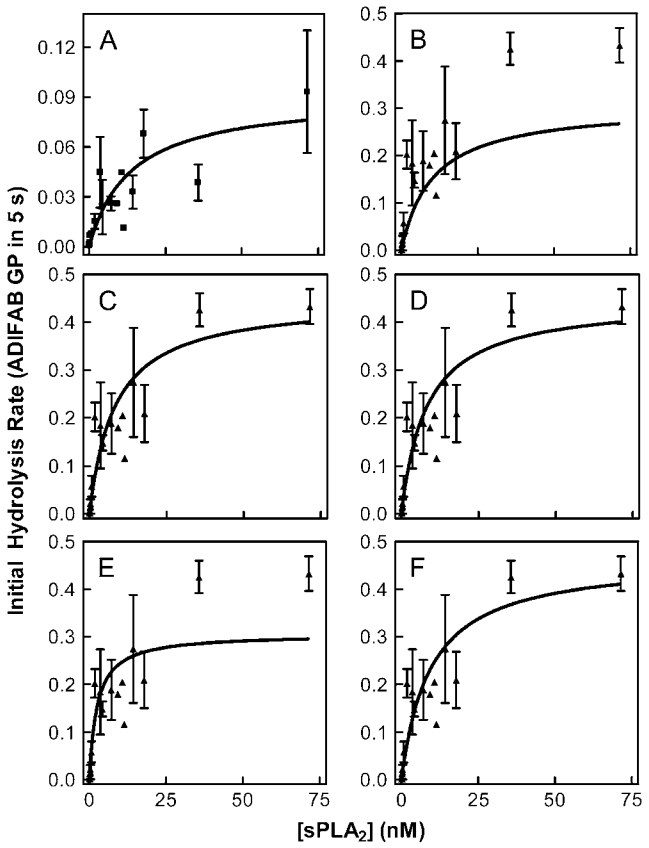

FIGURE 10 Analysis of hydrolysis results in terms of Scheme 1. Initial $sPLA_2$ hydrolysis rates from Fig. 2 *A* were fit by nonlinear regression to Eq. 2 multiple times with various combinations of constraints. (*A*) Baseline parameter values were obtained by fitting the control (DMSO) data from Fig. 2 *A*; parameter values are listed in the first row of Table 1. Some parameters were allowed to float in fits of the ionomycin data (*B–F*), as detailed below. S_T was fixed at 1.0 GP units in *A* and at 4.66 GP units with the ionomycin data (except in *C*), as explained in the text. The remaining parameters were kept fixed at the values obtained in *A* (details in Table 1, *rows 2–6*). The parameters allowed to float during the fits for each panel were: (*B*) no parameters, (*C*) S_T, (*D*) K_E, (*E*) K_A, and (*F*) K_E and K_A.

have been identified which differ in their intrinsic catalytic activity (k_{cat}), their affinity for membrane surfaces, and their dependence on the presence of anionic lipids (57). Thus, the degree to which phosphatidylserine exposure and potential differences in K_A contribute to the level of membrane hydrolysis under different experimental or physiological conditions may well depend on the isoform in question. Nevertheless, in previous experiments, human groups IIa and V $sPLA_2$ species displayed behavior toward S49 cells that was qualitatively identical to that observed with the snake venom enzyme (27). Therefore, although quantitative differences exist among various $sPLA_2$ types, the concept that substrate availability contributes, at least in part, to the level of membrane susceptibility probably applies to all of them.

Structural evidence suggests that $sPLA_2$ acts at the membrane surface with its active site displaced physically from the position normally occupied by bilayer phospholipids

TABLE 1 Parameter values for interaction between $sPLA_2$ and cell membranes

	Parameters			
Fig. 10 panel	β (GP units s^{-1})	K_A (nM^{-1})	K_E	S_T (relative units)
A	1.0	0.067	0.10	1.0
B	1.0	0.067	0.10	4.43
C	1.0	0.067	0.10	**8.12**
D	1.0	0.067	**0.18**	4.43
E	1.0	**0.273**	0.10	4.43
F	1.0	**0.056**	**0.20**	4.43

Parameter values were obtained by nonlinear regression using Eq. 2, as explained in the legend to Fig. 10. Values allowed to float in the regression are in bold print.

(24). If this is true, substrate availability (S_T) represents the number of lipids capable of making a vertical movement from their normal position, which, according to the results (Fig. 2 *B*), increases during a sustained calcium influx. Moreover, the larger value of K_E required to fit the data indicates that this vertical transition also occurs more easily.

We focused our analysis primarily on the initial rate of hydrolysis to avoid concerns about latent hydrolysis of internal bilayers such as the perinuclear membrane (36,37). Of course, measurement of total hydrolysis would include any internal hydrolysis product generated during the 10-min time frame of the experiment (see Fig. 2 *B*), especially with ionomycin treatment, which promoted internalization of L-PLA_2 (see Fig. 3 *B*). Therefore, it may be unreasonable to include the full measured value of S_T in the analysis with Eq. 2. The observation that the majority of total hydrolysis to be accomplished is complete within ~50 s (Fig. 1) mitigates this concern since this timescale is shorter than that reported for internalization (36,37). Based on the linkage of K_E and S_T in Eq. 2, overestimation of S_T corresponds to underestimation of K_E; thus, changes in K_E may be greater than we assumed in the analysis shown in Fig. 10 and Table 1. Regardless of the relative contributions of those two parameters to the effect of ionomycin on the initial rate, the argument that the membrane properties have changed to facilitate availability of substrate (either kinetically, K_E, or physically, S_T) to the active site of the enzyme is still valid. Obviously, the mechanistic basis for increased S_T in the presence of ionomycin requires additional investigation.

What could account for the increase in substrate access to the enzyme? The fluorescence of three of the five membrane probes we examined changed reproducibly due to ionophore. For example, MC540 bound more easily to the membrane, and laurdan emission was red-shifted, consistent with increased penetration of water molecules into the bilayer. These two observations suggest that the membrane surface had become more accommodating to intercalation of contaminating molecules from the aqueous phase. This result, together with an enhanced rate of NBD-PC extraction from the outer leaflet of the cell membrane, implies that the strength of interaction

among neighboring phospholipids is diminished by calcium influx. With the loss of favorable interactions coupled with increased hydration of the bilayer, the hydrophobic active site of the enzyme would presumably become a more attractive alternative to the membrane, thus enhancing the probability of hydrolysis.

Another possible explanation for the laurdan fluorescence relates to phospholipid chain dynamics. Many studies have suggested that changes in solvent access to laurdan correlate with the level of phospholipid chain order (32,33,58–60). The experiments conducted with bis-pyrene and DPH allowed us to examine whether such was the case here, since both probes are sensitive to the order of their environment (44). Interestingly, neither probe detected any change associated with ionomycin treatment. Therefore, the average level of phospholipid chain order in the membrane appeared to remain stable during calcium influx, and our interpretation of laurdan fluorescence relating to hydration changes at the membrane surface appears more plausible.

Initially, it may seem counterintuitive to propose that disruptive alterations have occurred that can be detected readily at the membrane surface without removing constraints on probe motion deep in the bilayer. One possibility is that ionophore treatment has generated local regions of high curvature stress in the membrane causing an increase in headgroup spacing simultaneous with crowding of the chains. Since phospholipid micelles are excellent substrates for $sPLA_2$ (61), such local curvature could explain the various observations in this report. We also note that changes in lipid spacing can occur without accompanying alterations in lipid order and/or lipid fluidity within liquid-ordered phases in both erythrocytes and artificial membranes (44).

This result (alterations at the surface with no change in chain order) contrasts observations from erythrocytes in which treatment with ionomycin actually increased the average lipid order of the membrane (18–20). Two distinctions between erythrocytes and lymphocytes are helpful in understanding this difference. First, susceptibility to hydrolysis upon ionophore treatment is about six times greater in lymphocytes than in erythrocytes (compare data in Fig. 2 to Smith et al. (18)). Logically, one would expect that membrane changes relevant to hydrolysis would also be more prominent in S49 cells. Changes observed in laurdan GP and MC540 fluorescence intensity were enhanced by factors of $\sim$10 (in the opposite direction) and 70, respectively, fulfilling this criterion (compare data in this report with raw data used in Best et al. (20) and Jensen et al. (21)). Second, microscopic images of erythrocytes revealed that ionomycin-induced alterations in lipid order were confined to specific membrane domains (18,20). In general, membrane domains in nucleated cells are much smaller than those of erythrocytes (62), making it unlikely that similar observations of increased order in discrete domains would be possible in lymphocytes, especially against the background of a more pronounced membrane hydration described above. Nevertheless, it is important to note that the data described for erythrocytes led to the same conclusion as that inferred here: that increased susceptibility to enzyme hydrolysis is precipitated by a reduction in the strength of lipid-neighbor interactions.

A major remaining question is the means by which ionophore treatment produces membrane changes responsible for elevated $sPLA_2$ activity. Resolution of this matter will require genetic and biochemical approaches beyond the scope of this study. Nevertheless, possible candidates may be identified from existing reports. The fact that cells rapidly become susceptible to $sPLA_2$ (i.e., within 10 min) during ionomycin-induced apoptosis helps evaluate the possibilities and exclude those events that arise too late (9). One obvious candidate for linking known apoptotic events with membrane sensitivity to $sPLA_2$ is the exposure of phosphatidylserine. As discussed above, this event appears unable to explain the increase in membrane hydrolysis, at least for the snake venom enzyme. Membrane blebbing and loss of integrity can also be eliminated as major contributing factors, because these events occur much later than the onset of susceptibility (9). The images in Figs. 7 and 9 corroborate the observation with respect to blebbing. The sustained loss of membrane potential associated with ionophore- and hormone-induced apoptosis in lymphocytes also appears to occur on a timescale well beyond that relevant to the phospholipase (3,5).

Ceramide accumulation, through de novo synthesis and cleavage of sphingomyelin, is well established as a participant in apoptotic signaling pathways (2). Furthermore, it has been suggested that sphingomyelin inhibits $sPLA_2$, and that its removal could therefore promote increased activity of the enzyme (63,64). The details of ceramide's role in apoptosis vary among cell types (2) and have not yet been characterized in S49 cells. Nonetheless, in prior experiments, treatment of S49 cells with sphingomyelinase did not enhance $sPLA_2$ activity (27).

In addition to blebbing, apoptotic cells sometimes shed smaller pieces of the plasma membrane known as microvesicles. Such is the case with ionomycin-stimulated S49 cells (27). This microvesiculation appears to be facilitated by both phosphatidylserine exposure and cytoskeletal cleavage, and the vesicles released are susceptible to the enzyme (18,63,65–68). These observations raise the question of whether the increase in membrane susceptibility reflects direct hydrolysis of the plasma membrane or, instead, degradation of released microvesicles. This issue has been addressed extensively in studies of human erythrocytes and S49 cells. In both cases, the conclusion was reached that although microvesicles are attacked by the enzyme, they represent a minor fraction of the total hydrolysis, with the remainder occurring in membranes associated with the cells (18,27).

Cytoskeletal alterations are more likely candidates for apoptotic events that might alter the membrane's response to $sPLA_2$ (6–8). Given the sensitivity of various membrane properties to cytoskeletal structure during apoptosis (6), it is

reasonable to speculate that the same may be true for the response to $sPLA_2$. For example, membrane tension could be highly important in determining the access of lipids to the enzyme active site (22) and certainly would be affected by the arrangement and number of cytoskeletal attachments. Likewise, cytoskeletal elements may regulate the lateral distribution of membrane lipids. Disruption of domain structure upon cytoskeletal rearrangement could free additional substrate for catalysis that previously was inaccessible to the enzyme (thus, the increase in S_T). We are now initiating genetic, pharmacological, and histological studies to explore these interesting possibilities as well as the relationship to other membrane events discussed here.

The long-term goal of this line of research is an understanding of the relationship between cell membrane structure and the differential activity of $sPLA_2$ in physiological settings. To that end, this report applies the model of $sPLA_2$ action developed by multiple researchers (see Scheme 1) to nucleated cells to test hypotheses derived from erythrocyte studies. Erythrocytes were employed in those prior studies because they offer a simplified, quasicellular model devoid of certain experimental complications, such as probes binding to intracellular membranes. Fortunately, we were able to address these complications here using flow cytometry and two-photon microscopy to assist in the interpretation of the data (see Results). The move to lymphocytes was a meaningful step toward a biologically relevant system in which susceptibility to $sPLA_2$ occurs during physiological processes such as apoptosis. Most important, we have demonstrated means by which biophysical techniques and information regarding membrane-protein interactions can be applied to studies of nucleated cells. The next step will be to resolve the timing of the membrane changes described in this report with respect to both the level of sensitivity to $sPLA_2$ and other events during hormone-stimulated apoptosis.

We gratefully acknowledge technical assistance from Summer King, Aubrielle Williamsen, Anne Heiner, Thaothanh Nguyen, Jennifer Nelson, and Chisako McLemore. Two-photon images were acquired at the Laboratory for Fluorescence Dynamics at the University of California, Irvine. We express thanks to the LFD staff, especially Susana Sanchez, Theodore Hazlett, and the director of the facility, Enrico Gratton, for their assistance. Flow cytometry experiments were conducted with the assistance of Sandra Burnett and Nels Nielson at the Research Instrumentation Core Facility at Brigham Young University.

This work was supported by the National Institutes of Health (GM073997).

REFERENCES

1. Arnold, R., D. Brenner, M. Becker, C. R. Frey, and P. H. Krammer. 2006. How T lymphocytes switch between life and death. *Eur. J. Immunol.* 36:1654–1658.
2. Taha, T. A., T. D. Mullen, and L. M. Obeid. 2006. A house divided: ceramide, sphingosine, and sphingosine-1-phosphate in programmed cell death. *Biochim. Biophys. Acta.* 1758:2027–2036.
3. Bortner, C. D., M. Gomez-Angelats, and J. A. Cidlowski. 2001. Plasma membrane depolarization without repolarization is an early molecular event in anti-Fas-induced apoptosis. *J. Biol. Chem.* 276:4304–4314.
4. Mann, C. L., C. D. Bortner, C. M. Jewell, and J. A. Cidlowski. 2001. Glucocorticoid-induced plasma membrane depolarization during thymocyte apoptosis: association with cell shrinkage and degradation of the Na^+/Ks^+-adenosine triphosphatase. *Endocrinology.* 142:5059–5068.
5. Mann, C. L., and J. A. Cidlowski. 2001. Glucocorticoids regulate plasma membrane potential during rat thymocyte apoptosis in vivo and in vitro. *Endocrinology.* 142:421–429.
6. Martin, S. J., D. M. Finucane, G. P. Amarante-Mendes, G. A. O'Brien, and D. R. Green. 1996. Phosphatidylserine externalization during CD95-induced apoptosis of cells and cytoplasts requires ICE/CED-3 protease activity. *J. Biol. Chem.* 271:28753–28756.
7. LeDuc, P. P., and R. R. Bellin. 2006. Nanoscale intracellular organization and functional architecture mediating cellular behavior. *Ann. Biomed. Eng.* 34:102–113.
8. Coleman, M. L., and M. F. Olson. 2002. Rho GTPase signalling pathways in the morphological changes associated with apoptosis. *Cell Death Differ.* 9:493–504.
9. Nielson, K. H., C. A. Olsen, D. V. Allred, K. L. O'Neill, G. F. Burton, and J. D. Bell. 2000. Susceptibility of S49 lymphoma cell membranes to hydrolysis by secretory phospholipase A(2) during early phase of apoptosis. *Biochim. Biophys. Acta.* 1484:163–174.
10. Atsumi, G., M. Murakami, M. Tajima, S. Shimbara, N. Hara, and I. Kudo. 1997. The perturbed membrane of cells undergoing apoptosis is susceptible to type II secretory phospholipase A2 to liberate arachidonic acid. *Biochim. Biophys. Acta.* 1349:43–54.
11. Henshaw, J. B., C. A. Olsen, A. R. Farnbach, K. H. Nielson, and J. D. Bell. 1998. Definition of the specific roles of lysolecithin and palmitic acid in altering the susceptibility of dipalmitoylphosphatidylcholine bilayers to phospholipase A2. *Biochemistry.* 37:10709–10721.
12. Gelb, M. H., M. K. Jain, A. M. Hanel, and O. G. Berg. 1995. Interfacial enzymology of glycerolipid hydrolases: lessons from secreted phospholipases A2. *Annu. Rev. Biochem.* 64:653–688.
13. Berg, O. G., J. Rogers, B. Z. Yu, J. Yao, L. S. Romsted, and M. K. Jain. 1997. Thermodynamic and kinetic basis of interfacial activation: resolution of binding and allosteric effects on pancreatic phospholipase A2 at zwitterionic interfaces. *Biochemistry.* 36:14512–14530.
14. Yu, B. Z., M. J. Poi, U. A. Ramagopal, R. Jain, S. Ramakumar, O. G. Berg, M. D. Tsai, K. Sekar, and M. K. Jain. 2000. Structural basis of the anionic interface preference and kcat* activation of pancreatic phospholipase A2. *Biochemistry.* 39:12312–12323.
15. Honger, T., K. Jorgensen, D. Stokes, R. L. Biltonen, and O. G. Mouritsen. 1997. Phospholipase A2 activity and physical properties of lipid-bilayer substrates. *Methods Enzymol.* 286:168–190.
16. Burack, W. R., A. R. Dibble, M. M. Allietta, and R. L. Biltonen. 1997. Changes in vesicle morphology induced by lateral phase separation modulate phospholipase A2 activity. *Biochemistry.* 36:10551–10557.
17. Tatulian, S. A. 2001. Toward understanding interfacial activation of secretory phospholipase A2 (PLA2): membrane surface properties and membrane-induced structural changes in the enzyme contribute synergistically to PLA2 activation. *Biophys. J.* 80:789–800.
18. Smith, S. K., A. R. Farnbach, F. M. Harris, A. C. Hawes, L. R. Jackson, A. M. Judd, R. S. Vest, S. Sanchez, and J. D. Bell. 2001. Mechanisms by which intracellular calcium induces susceptibility to secretory phospholipase A2 in human erythrocytes. *J. Biol. Chem.* 276:22732–22741.
19. Harris, F. M., S. K. Smith, and J. D. Bell. 2001. Physical properties of erythrocyte ghosts that determine susceptibility to secretory phospholipase A2. *J. Biol. Chem.* 276:22722–22731.
20. Best, K., A. Ohran, A. Hawes, T. L. Hazlett, E. Gratton, A. M. Judd, and J. D. Bell. 2002. Relationship between erythrocyte membrane phase properties and susceptibility to secretory phospholipase A2. *Biochemistry.* 41:13982–13988.
21. Jensen, L. B., N. K. Burgess, D. D. Gonda, E. Spencer, H. A. Wilson-Ashworth, E. Driscoll, M. P. Vu, J. L. Fairbourn, A. M. Judd, and J. D. Bell. 2005. Mechanisms governing the level of susceptibility of erythrocyte membranes to secretory phospholipase A2. *Biophys. J.* 88: 2692–2705.

22. Verger, R., M. C. Mieras, and G. H. de Haas. 1973. Action of phospholipase A at interfaces. *J. Biol. Chem.* 248:4023–4034.

23. Sheffield, M. J., B. L. Baker, D. Li, N. L. Owen, M. L. Baker, and J. D. Bell. 1995. Enhancement of *Agkistrodon piscivorus piscivorus* venom phospholipase A2 activity toward phosphatidylcholine vesicles by lysolecithin and palmitic acid: studies with fluorescent probes of membrane structure. *Biochemistry.* 34:7796–7806.

24. Scott, D. L., S. P. White, Z. Otwinowski, W. Yuan, M. H. Gelb, and P. B. Sigler. 1990. Interfacial catalysis: the mechanism of phospholipase A2. *Science.* 250:1541–1546.

25. Burack, W. R., and R. L. Biltonen. 1994. Lipid bilayer heterogeneities and modulation of phospholipase A2 activity. *Chem. Phys. Lipids.* 73: 209–222.

26. Yu, B. Z., O. G. Berg, and M. K. Jain. 1993. The divalent cation is obligatory for the binding of ligands to the catalytic site of secreted phospholipase A2. *Biochemistry.* 32:6485–6492.

27. Wilson, H. A., J. B. Waldrip, K. H. Nielson, A. M. Judd, S. K. Han, W. Cho, P. J. Sims, and J. D. Bell. 1999. Mechanisms by which elevated intracellular calcium induces S49 cell membranes to become susceptible to the action of secretory phospholipase A2. *J. Biol. Chem.* 274:11494–11504.

28. Wilson, H. A., W. Huang, J. B. Waldrip, A. M. Judd, L. P. Vernon, and J. D. Bell. 1997. Mechanisms by which thionin induces susceptibility of S49 cell membranes to extracellular phospholipase A2. *Biochim. Biophys. Acta.* 1349:142–156.

29. Maraganore, J. M., G. Merutka, W. Cho, W. Welches, F. J. Kezdy, and R. L. Heinrikson. 1984. A new class of phospholipases A2 with lysine in place of aspartate 49. Functional consequences for calcium and substrate binding. *J. Biol. Chem.* 259:13839–13843.

30. Dam-Mieras, M. C., A. J. Slotboom, W. A. Pieterson, and G. H. de Haas. 1975. The interaction of phospholipase A2 with micellar interfaces. The role of the N-terminal region. *Biochemistry.* 14:5387–5394.

31. Yu, B. Z., J. Rogers, G. R. Nicol, K. H. Theopold, K. Seshadri, S. Vishweshwara, and M. K. Jain. 1998. Catalytic significance of the specificity of divalent cations as KS* and kcat* cofactors for secreted phospholipase A2. *Biochemistry.* 37:12576–12587.

32. Parasassi, T., G. De Stasio, G. Ravagnan, R. M. Rusch, and E. Gratton. 1991. Quantitation of lipid phases in phospholipid vesicles by the generalized polarization of laurdan fluorescence. *Biophys. J.* 60:179–189.

33. Harris, F. M., K. B. Best, and J. D. Bell. 2002. Use of laurdan fluorescence intensity and polarization to distinguish between changes in membrane fluidity and phospholipid order. *Biochim. Biophys. Acta.* 1565:123–128.

34. Yu, W., P. T. So, T. French, and E. Gratton. 1996. Fluorescence generalized polarization of cell membranes: a two-photon scanning microscopy approach. *Biophys. J.* 70:626–636.

35. Murakami, M., T. Kambe, S. Shimbara, S. Yamamoto, H. Kuwata, and I. Kudo. 1999. Functional association of type IIA secretory phospholipase A(2) with the glycosylphosphatidylinositol-anchored heparan sulfate proteoglycan in the cyclooxygenase-2-mediated delayed prostanoid-biosynthetic pathway. *J. Biol. Chem.* 274:29927–29936.

36. Cho, W. 2000. Structure, function, and regulation of group V phospholipase A(2). *Biochim. Biophys. Acta.* 1488:48–58.

37. Kim, Y. J., K. P. Kim, H. J. Rhee, S. Das, J. D. Rafter, Y. S. Oh, and W. Cho. 2002. Internalized group V secretory phospholipase A2 acts on the perinuclear membranes. *J. Biol. Chem.* 277:9358–9365.

38. Lelkes, P. I., D. Bach, and I. R. Miller. 1980. Perturbations of membrane structure by optical probes: II. Differential scanning calorimetry of dipalmitoyllecithin and its analogs interacting with Merocyanine 540. *J. Membr. Biol.* 54:141–148.

39. Lelkes, P. I., and I. R. Miller. 1980. Perturbations of membrane structure by optical probes: I. Location and structural sensitivity of merocyanine 540 bound to phospholipid membranes. *J. Membr. Biol.* 52:1–15.

40. Onganer, Y., and E. L. Quitevis. 1994. Dynamics of merocyanine 540 in model biomembranes: photoisomerization studies in small unilamellar vesicles. *Biochim. Biophys. Acta.* 1192:27–34.

41. Lagerberg, J. W., K. J. Kallen, C. W. Haest, J. VanSteveninck, and T. M. Dubbelman. 1995. Factors affecting the amount and the mode of merocyanine 540 binding to the membrane of human erythrocytes. A comparison with the binding to leukemia cells. *Biochim. Biophys. Acta.* 1235:428–436.

42. Chong, P. L., and P. T. Wong. 1993. Interactions of laurdan with phosphatidylcholine liposomes: a high pressure FTIR study. *Biochim. Biophys. Acta.* 1149:260–266.

43. Melnick, R. L., H. C. Haspel, M. Goldenberg, L. M. Greenbaum, and S. Weinstein. 1981. Use of fluorescent probes that form intramolecular excimers to monitor structural changes in model and biological membranes. *Biophys. J.* 34:499–515.

44. Wilson-Ashworth, H. A., Q. Bahm, J. Erickson, A. Shinkle, M. P. Vu, D. Woodbury, and J. D. Bell. 2006. Differential detection of phospholipid fluidity, order, and spacing by fluorescence spectroscopy of bispyrene, prodan, nystatin, and merocyanine 540. *Biophys. J.* 91:4091–4101.

45. Vanderkooi, J. M., and J. B. Callis. 1974. Pyrene. A probe of lateral diffusion in the hydrophobic region of membranes. *Biochemistry.* 13: 4000–4006.

46. Kaiser, R. D., and E. London. 1998. Location of diphenylhexatriene (DPH) and its derivatives within membranes: comparison of different fluorescence quenching analyses of membrane depth. *Biochemistry.* 37:8180–8190.

47. Wang, S., J. M. Beechem, E. Gratton, and M. Glaser. 1991. Orientational distribution of 1,6-diphenyl-1,3,5-hexatriene in phospholipid vesicles as determined by global analysis of frequency domain fluorimetry data. *Biochemistry.* 30:5565–5572.

48. Williamson, P., A. Kulick, A. Zachowski, R. A. Schlegel, and P. F. Devaux. 1992. Ca^{2+} induces transbilayer redistribution of all major phospholipids in human erythrocytes. *Biochemistry.* 31:6355–6360.

49. Tatulian, S. A., R. L. Biltonen, and L. K. Tamm. 1997. Structural changes in a secretory phospholipase A2 induced by membrane binding: a clue to interfacial activation? *J. Mol. Biol.* 268:809–815.

50. Zhou, Q., J. Zhao, J. G. Stout, R. A. Luhm, T. Wiedmer, and P. J. Sims. 1997. Molecular cloning of human plasma membrane phospholipid scramblase. A protein mediating transbilayer movement of plasma membrane phospholipids. *J. Biol. Chem.* 272:18240–18244.

51. Bevers, E. M., P. Comfurius, and R. F. Zwaal. 1983. Changes in membrane phospholipid distribution during platelet activation. *Biochim. Biophys. Acta.* 736:57–66.

52. Jain, M. K., B. Z. Yu, and A. Kozubek. 1989. Binding of phospholipase A2 to zwitterionic bilayers is promoted by lateral segregation of anionic amphiphiles. *Biochim. Biophys. Acta.* 980:23–32.

53. Burack, W. R., Q. Yuan, and R. L. Biltonen. 1993. Role of lateral phase separation in the modulation of phospholipase A2 activity. *Biochemistry.* 32:583–589.

54. Murakami, M., T. Kambe, S. Shimbara, K. Higashino, K. Hanasaki, H. Arita, M. Horiguchi, M. Arita, H. Arai, K. Inoue, and I. Kudo. 1999. Different functional aspects of the group II subfamily (Types IIA and V) and type X secretory phospholipase A(2)s in regulating arachidonic acid release and prostaglandin generation. Implications of cyclooxygenase-2 induction and phospholipid scramblase-mediated cellular membrane perturbation. *J. Biol. Chem.* 274:31435–31444.

55. Koduri, R. S., S. F. Baker, Y. Snitko, S. K. Han, W. Cho, D. C. Wilton, and M. H. Gelb. 1998. Action of human group IIa secreted phospholipase A2 on cell membranes. Vesicle but not heparinoid binding determines rate of fatty acid release by exogenously added enzyme. *J. Biol. Chem.* 273:32142–32153.

56. Ashman, R. F., D. Peckham, S. Alhasan, and L. L. Stunz. 1995. Membrane unpacking and the rapid disposal of apoptotic cells. *Immunol. Lett.* 48:159–166.

57. Singer, A. G., F. Ghomashchi, C. Le Calvez, J. Bollinger, S. Bezzine, M. Rouault, M. Sadilek, M. Lazdunski, G. Lambeau, and M. H. Gelb. 2002. Interfacial kinetic and binding properties of the complete set of human and mouse groups I, II, V, X, and XII secreted phospholipases A2. *J. Biol. Chem.* 277:48535–48549.

58. Parasassi, T., G. Ravagnan, R. M. Rusch, and E. Gratton. 1993. Modulation and dynamics of phase properties in phospholipid mixtures detected by aurdan fluorescence. *Photochem. Photobiol.* 57:403–410.

59. Parasassi, T., M. Di Stefano, M. Loiero, G. Ravagnan, and E. Gratton. 1994. Influence of cholesterol on phospholipid bilayers phase domains as detected by Laurdan fluorescence. *Biophys. J.* 66:120–132.

60. Parasassi, T., A. M. Giusti, M. Raimondi, and E. Gratton. 1995. Abrupt modifications of phospholipid bilayer properties at critical cholesterol concentrations. *Biophys. J.* 68:1895–1902.

61. Verheij, H. M., A. J. Slotboom, and G. H. de Haas. 1981. Structure and function of phospholipase A2. *Rev. Physiol. Biochem. Pharmacol.* 91:91–203.

62. Parasassi, T., E. Gratton, W. M. Yu, P. Wilson, and M. Levi. 1997. Two-photon fluorescence microscopy of laurdan generalized polarization domains in model and natural membranes. *Biophys. J.* 72:2413–2429.

63. Fourcade, O., M. F. Simon, C. Viode, N. Rugani, F. Leballe, A. Ragab, B. Fournie, L. Sarda, and H. Chap. 1995. Secretory phospholipase A2 generates the novel lipid mediator lysophosphatidic acid in membrane microvesicles shed from activated cells. *Cell.* 80:919–927.

64. Koumanov, K., C. Wolf, and G. Bereziat. 1997. Modulation of human type II secretory phospholipase A2 by sphingomyelin and annexin VI. *Biochem. J.* 326:227–233.

65. Chang, C. P., J. Zhao, T. Wiedmer, and P. J. Sims. 1993. Contribution of platelet microparticle formation and granule secretion to the transmembrane migration of phosphatidylserine. *J. Biol. Chem.* 268:7171–7178.

66. Comfurius, P., J. M. Senden, R. H. Tilly, A. J. Schroit, E. M. Bevers, and R. F. Zwaal. 1990. Loss of membrane phospholipid asymmetry in platelets and red cells may be associated with calcium-induced shedding of plasma membrane and inhibition of aminophospholipid translocase. *Biochim. Biophys. Acta.* 1026:153–160.

67. Basse, F., P. Gaffet, and A. Bienvenue. 1994. Correlation between inhibition of cytoskeleton proteolysis and anti-vesiculation effect of calpeptin during A23187-induced activation of human platelets: are vesicles shed by filopod fragmentation? *Biochim. Biophys. Acta.* 1190:217–224.

68. Vest, R., R. Wallis, L. B. Jensen, A. C. Haws, J. Callister, B. Brimhall, A. M. Judd, and J. D. Bell. 2006. Use of steady-state laurdan fluorescence to detect changes in liquid ordered phases in human erythrocyte membranes. *J. Membr. Biol.* 211:15–25.